IEEE Access
Multidisciplinary | Rapid Review | Open Access Journal

Received 10 May 2023, accepted 27 May 2023, date of publication 31 May 2023, date of current version 7 June 2023.

Digital Object Identifier 10.1109/ACCESS.2023.3281691

RESEARCH ARTICLE

Repositioned Internal Model Control Strategy on Time-Delayed Industrial Processes With Inverse Behavior Using Equilibrium Optimizer

PULAKRAJ ARYAN[1], (Graduate Student Member, IEEE), G. LLOYDS RAJA[1], (Member, IEEE), RAMON VILANOVA[2], (Member, IEEE), AND MONTSE MENESES[2], (Member, IEEE)

[1]Electrical Engineering Department, National Institute of Technology Patna, Patna 800005, India
[2]Department of Telecommunications and Systems Engineering, Autonomous University of Barcelona, 08193 Barcelona, Spain

Corresponding authors: G. Lloyds Raja (lloyd.raja@gmail.com) and Ramon Vilanova (Ramon.Vilanova@uab.cat)

This work was supported in part by the Catalan Government under Project 2021 SGR 00197, and in part by the Spanish Government co-funded with the European Union ERDF funds through MICINN Project under Grant PID2019-105434RBC33 and Grant TED2021-806129134B-I00.

ABSTRACT This paper investigates a repositioned inner-loop stabilized internal model control technique for demanding inverse response industrial processes and bioreactors with integrating/unstable dynamics. A proportional-derivative controller based on Routh stability principles is used to achieve stabilization. For set-point pursuit, the servo controller is built by applying the relocation internal model control principle to the stabilized plant model. The metaheuristic equilibrium optimizer methodology is used to achieve the optimal controller settings of the proposed method. The recommended technique is investigated for managing inverse response processes such as the steam drum level control system, concentration in enzymatic reactors, and continuously stirred tank reactors. A thorough examination of the proposed scheme's stability and robust performance is also provided. It provides significant improvement in performance metrics when compared with some of the recently reported strategies. Particularly, for the steam drum system, the suggested strategy yields an improvement of over 47% in the disturbance rejection and more than three times faster servo response when compared with the recently reported integral proportional-derivative double control loop strategy.

INDEX TERMS Inner-loop stabilization, repositioned internal model control, integrating and unstable processes, inverse response, time delay, equilibrium optimizer.

NOMENCLATURE

β	Delay value.
δ	Input disturbance.
$\hat{G}_{ILS}$	Repositioned ILS transfer function.
ρ	Volumetric surge.
C_{eqb}	Equilibrium concentration.
C_{ILS}	ILS controller.
G	Plant model.
G_f	Filter transfer function.
G_r	Generation rate.
G_{ILS}	ILS transfer function.
K_d	Derivative gain.
K_P	Proportional gain.
R	Reference.
T_{st}	Settling time.
U	Control effort.
V	Control confinement.
Y	Plant output.
DCL	Double control loop.
DS	Direct synthesis.
EO	Equilibrium optimizer.
IAE	Integral absolute error.
ILS	Inner-loop stablization.

The associate editor coordinating the review of this manuscript and approving it for publication was Nasim Ullah.

This work is licensed under a Creative Commons Attribution-NonCommercial-NoDerivatives 4.0 License.
For more information, see https://creativecommons.org/licenses/by-nc-nd/4.0/

IMC	Internal model control.
ISE	Integral square error.
ITAE	Integral time absolute error.
ITSE	Integral time square error.
NMP	Non-minimum phase.
RH	Routh Hurwitz.
SCL	Single control loop.
TD	Time delay.
UIP	Unstable and integrating processes.

I. INTRODUCTION

A. BACKGROUND OF STUDY

Processes with unstable dynamics are commonly witnessed in industries involving chemical reactors, boilers, heat radiators etc. [1]. Meanwhile, the dynamics of distillation columns, liquid storage with an attached pump, drier cans of the paper industry etc. are of integrating nature [2], [3]. Unstable and integrating processes (UIPs) are non-self-regulating in nature due to which they fail to stabilize after the introduction of any arbitrary disturbance. There is an inherent presence of time delay (TD) in the majority of these processes which arises due velocity lag, transfer and recycle loops [4], composition investigation [1], [5], network-induced [6] etc. TD introduces additional phase lag in the system. Non-minimum phase (NMP) / inverse response industrial processes respond in the opposing direction to the control effort. The existence of NMP characteristics makes the UIPs with TD even more challenging. In such instances, the controlled variable may drop for a while before rising again. In complex frequency plane interpretation, the inverse response phenomenon occurs due to the existence of open-loop zero(s) in the right half of the plane. For such processes, the double control loop (DCL) structures are more effective control strategies than the single control loop (SCL) [5], [7], [8], [9].

B. RELATED WORKS

SCL schemes are widely used due to their simplicity in design. PI/PID are the popular controllers used in SCL schemes. For controlling bioreactors of unstable nature, [10] utilized a PI controller alongside an unstable filter. The popular approaches for designing a PID controller include direct synthesis (DS) [11], [12], [13], [14], [15], desired characteristic equation matching [16], error function minimization [17] and internal model control (IMC) based design [18], [19], [20], [21], [22]. Some other PID design approaches used by researchers are the weighted performance degradation method [15] and H2 minimization [23]. Figure 1 reveals the SCL and DCL structures. The structure of the DCL is similar to that of a unity feedback SCL scheme except for the presence of an additional inner-loop in the DCL. This is responsible for stabilizing the plant (called the inner-loop stabilization or ILS) before subjecting it to the outer-loop control which helps in attaining the reference pursuance. Additionally, ILS is also responsible for mitigating the effect of disturbance.

The DCL design was initially devised by Park et al. [24] for unstable processes. Vijayan and Panda [25] designed PID using the IMC method along with the proportional ILS controller tuned using Ziegler-Nichol's method. A Smith-predictor (SP) was utilized with DCL by Cong et al. [26] for controlling unstable plants. SP serves as the dead-time compensator for delay-dominant processes in the above-cited approach. Ajmeri and Ali [27] presented a double-degree of freedom (2-Dof) control method for unstable processes as an improvement of the parallel control architecture. PI-PD is a prevalent DCL scheme [7], [28], [29], [30], [31] in which the PID is replaced with PI while PD performs the ILS. In the PI-PD structure proposed by Li [28], the controllers were designed using the model predictive control (MPC) approach. Onat [29], Alyoussef and Kaya [30], [31] used graphical methods to find their respective PI-PD stabilization regions. Routh-Hurwitz (RH) criteria and moment matching technique were utilized by Raja and Ali [7] to design their PI-PD scheme. The PI-PD structure is further modified to I-PD DCL scheme by a few researchers [9], [32], [33]. Very recently, Doğruer [34] used a modified SP-based I-PD scheme for controlling inverse response processes. However, the above-cited work involves two heuristically-tuned PD controllers in contrast to traditional DCLs.

The IMC-based DCLs have attracted good research attention in recent times. Aryan and Raja [2] used the IMC-PD DCL scheme for controlling UIPs in which the controller settings were determined using the equilibrium optimizer (EO). Kumari et al. [5] replaced the IMC with fractional-order IMC (FOIMC) in their DCL structure alongside the P/PD ILS scheme for controlling the unstable continuous stirred tank reactor (CSTR). Kumar et al. [35] modified the DCL structure of Kumari et al. [5] into a decoupled FOIMC-PD architecture for controlling processes with a double pole at the origin (double integral processes).

C. HEURISTIC ALGORITHMS

Heuristic algorithms produce and make use of random variables [36]. They are not dependent on the nature of the problem, unlike deterministic approaches, because they do not require mathematical details of the problem [37]. These methods are gaining popularity due to their adaptability, which allows them to solve any sort of optimisation problem without modifying the algorithm's structure. The ability to escape local optima with exploration and exploitation features is also significant [38]. The prominent ones to fall in this category include grey wolf optimization [36], Sine-cosine algorithm [37] and moth-flame optimization algorithm [38]. These algorithms have registered significant presence in economic dispatch problems [39], [40], [41], [42]. The notable ones include simulated annealing hybridized with sequential quadratic programming (SQP) [39], astute black widow

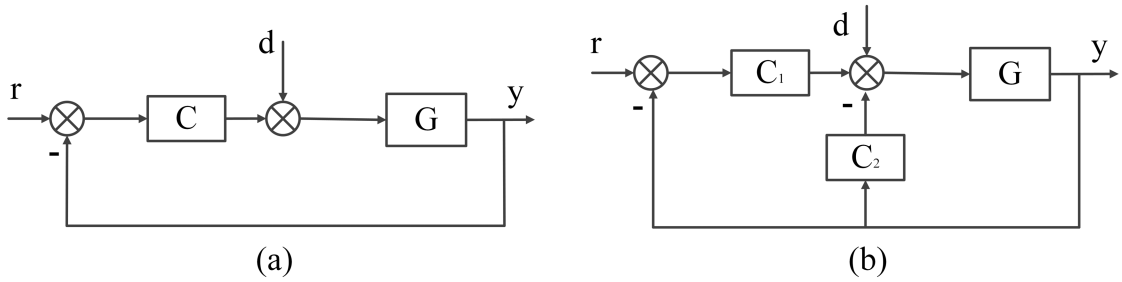

FIGURE 1. Controller schemes (a) SCL (b) DCL.

optimization [40], whale optimization [41] and genetic algorithm-based SQP [42].

Among the metaheuristic techniques available of late, EO has emerged as a prominent algorithm since its inception by Faramarzi et al. [43]. Predominantly used for load frequency control methods [44], [45], EO has now gained popularity in process control applications [1], [2], [34], [46] with its ability to simultaneously tune multi-parameters to achieve the desired performance.

D. KEY RESEARCH GAP AND MOTIVATION

The optimal control strategies produce enhanced performance measures but the robustness is compromised. Verma and Padhy [20] introduced the concept of indirect or repositioned IMC-based PID in SCL configuration for controlling stable processes. The repositioned IMC (RIMC) was able to provide a decent robustness-performance tradeoff. Very recently, Aryan et al. [1] introduced RIMC in DCL for controlling time-delayed UIPs. However, the aforementioned literature was limited to controlling only minimum phase UIPs. So, there is a need to redesign RIMC-based strategy for challenging inverse response processes.

E. RESEARCH OBJECTIVE AND CONTRIBUTION

In this work, the DCL strategy reported by Aryan et al. [1] is redesigned to present a unified approach so that it can be applied to NMP UIPs. The RIMC and ILS controllers are constructed following the RH stability guidelines and the relocation principle. The optimal controller settings are then determined by the EO. The usage of both RIMC (a robust controller design method) and EO (a recently reported advanced metaheuristic algorithm) ensures a better performance-robustness tradeoff than the existing solutions reported for the problems posed by inverse response plants. The suggested control strategy is investigated for controlling challenging inverse response UIPs such as the steam drum level control system and concentration in enzymatic reactor along with continuous stirred tank reactor (CSTR). A comprehensive robust performance assessment and stability analysis of the suggested ILS-RIMC scheme is also presented. The main contributions of this work are divulged below:

- Maiden application of ILS-based RIMC control strategy for inverse response UIPs with TD tuned using metaheuristic EO.
- Simulation studies are conducted on benchmark inverse response plant models such as the level control system, bioreactor concentration control and CSTR which show significant improvement in the performance measures achieved by the suggested design over recently reported SCL and DCL strategies.

Rest of the manuscript is structured in following manner: Control scheme is discussed in section II. EO is studied in section III. Results of the simulations are detailed in section IV. The conclusive summary and future scope of the suggested work is presented in section V.

II. CONTROL SCHEME

A typical second-order NMP UIP [47] with a TD of β is given as

$$G(s) = \frac{\sum_{i=0}^{1} a_i(-s)^i}{\sum_{i=0}^{2} b_i s^i} e^{-\beta s} = \frac{(a_0 - a_1 s)}{b_2 s^2 + b_1 s + b_0} e^{-\beta s} \quad (1)$$

For $a_0 = 1$ and $a_1 > 0$, (1) exhibits inverse response characteristics with a positive zero located at $s = 1/a_1$. Based on denominator coefficients b_2, b_1 and b_0, (1) illustrates the following class of commonly encountered processes:

1) U1PTD* for $b_0 < 0, b_2 = 0$
2) I2PTD** for $b_0 = 0, b_1 > 0$
3) U2PTD*** for $0 < a_1 < a_2, a_0 = -1$

U1PTD*-unstable first order plus time delay, I2PTD**- integrating second order plus time delay, U2PTD***- unstable second order plus time delay

Figure 2 depicts the suggested ILS-RIMC control scheme having controllers C_{ILS} and C_{RIMC}. Here, 'R' is the applied reference signal while 'Y' is the plant (G) output. R' can be treated as the augmented reference to the ILS transfer function (G_{ILS}) while 'U' is the control effort. 'δ' denotes the input disturbance entering the plant. $\hat{G}_{ILS}$ is obtained after repositioning G_{ILS} by θ. The expressions for C_{ILS} and C_{RIMC} are derived in the following subsections:

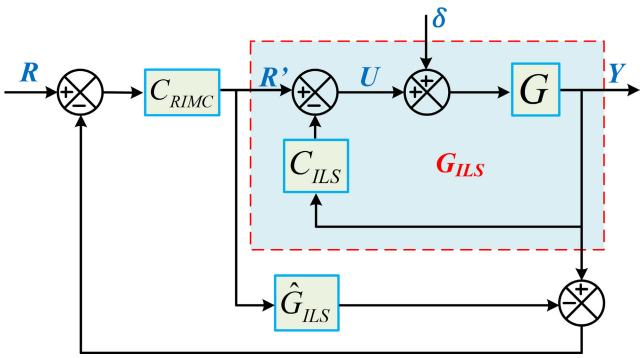

FIGURE 2. The suggested ILS-RIMC control structure.

A. ILS CONTROLLER

Inner-loop stabilization is achieved by utilizing the PD [7] controller given by

$$C_{ILS}(s) = K_P + K_d s \tag{2}$$

From Figure 2, the ILS transfer function can be obtained as

$$G_{ILS}(s) = \frac{Y(s)}{R'(s)} = \frac{G(s)}{1 + G(s)\,C_{ILS}(s)} \tag{3}$$

Utilizing (1) and (2) in (3) gives

$$G_{ILS}(s) = \frac{\frac{(a_0 - a_1 s)}{b_2 s^2 + b_1 s + b_0} e^{-\beta s}}{1 + \frac{(a_0 - a_1 s)}{b_2 s^2 + b_1 s + b_0} e^{-\beta s} \times (K_P + K_d s)} \tag{4}$$

(4) can be rearranged as

$$G_{ILS}(s) = \frac{(a_0 - a_1 s)\, e^{-\beta s}}{\left\{ \begin{array}{l} \left(b_2 s^2 + b_1 s + b_0\right) \\ +\, (a_0 - a_1 s)\, e^{-\beta s} \times (K_P + K_d s) \end{array} \right\}} \tag{5}$$

As (5) contains an exponential term in the denominator, it needs to be linearized to proceed with the stability constraints.

1) CASE 1: USING PADE's 1st ORDER APPROXIMATION

In this case, $e^{-\beta s}$ is approximated by $\left(\frac{1-0.5\beta s}{1+0.5\beta s}\right)$ [48] yielding the following expression:

$$G_{ILS}(s) = \frac{(a_0 - a_1 s)\, e^{-\beta s}}{\left\{ \begin{array}{l} \left(b_2 s^2 + b_1 s + b_0\right) + (a_0 - a_1 s) \\ \frac{1-0.5\beta s}{1+0.5\beta s} \times K_P \left(1 + \frac{K_d}{K_P} s\right) \end{array} \right\}} \tag{6}$$

If $(1 + 0.5\beta s)$ is to be canceled with $\left(1 + \frac{K_d}{K_P} s\right)$, then

$$\frac{K_d}{K_P} = 0.5\beta \tag{7}$$

Using (7) in (6) results in the following:

$$G_{ILS}(s) = \frac{(a_0 - a_1 s)\, e^{-\beta s}}{\left\{ \begin{array}{l} \left(b_2 + 0.5\beta a_1 K_P\right) s^2 \\ +\, \left(b_1 - 0.5\beta a_0 K_P - a_1 K_P\right) s \\ +\, b_0 + a_0 K_P \end{array} \right\}} \tag{8}$$

Finally, the ILS transfer function can be given as

$$G_{ILS}(s) = \frac{(a_0 - a_1 s)}{c_2 s^2 + c_1 s + c_0} e^{-\beta s} = \frac{\sum_{i=0}^{1} a_i (-s)^i}{\sum_{i=0}^{2} c_i s^i} e^{-\beta s} \tag{9}$$

where, $c_2 = \left(b_2 + 0.5\beta a_1 K_P\right)$, $c_1 = \left(b_1 - 0.5\beta a_0 K_P - a_1 K_P\right)$ and $c_0 = \left(b_0 + a_0 K_P\right)$. Subjecting (8) to R-H stability analysis gives the following relations:

$$\left. \begin{array}{c} K_P > \frac{-2b_2}{\beta a_1} \\ K_P < \frac{b_1}{0.5\beta a_0 + a_1} \\ K_P > \frac{-b_0}{a_0} \end{array} \right\} \tag{10}$$

The above constraints hold true for both minimum and non-minimum phase systems.

2) CASE 2: USING PADE's 2nd ORDER APPROXIMATION

In this case, $e^{-\beta s}$ is approximated by $\left(\frac{6-2\beta s}{6-4\beta s+\beta^2 s^2}\right)$ [48] yielding the following expression:

$$G_{ILS}(s) = \frac{(a_0 - a_1 s) e^{-\beta s}}{\left(\begin{array}{l} \left(b_2 s^2 + b_1 s + b_0\right) + (a_0 - a_1 s) \\ \times \left(\frac{6-2\beta s}{6-4\beta s+\beta^2 s^2}\right) \times (K_P + K_d s) \end{array} \right)} \tag{11}$$

If $(6-4\beta s+\beta^2 s^2)$ is to be canceled with $(6-2\beta s)(K_P+K_d s)$, then

$$\left. \begin{array}{l} K_P = 1 \\ K_d = -\frac{\beta}{2} \end{array} \right\} \tag{12}$$

Using (12) in (11) results in the following:

$$G_{ILS}(s) = \frac{(a_0 - a_1 s) e^{-\beta s}}{\left(b_2 s^2 + (b_1 - a_1)\, s + b_0 + a_0\right)} \tag{13}$$

Finally, the ILS transfer function in this case can be once again given as (9) with $c_2 = b_2$, $c_1 = (b_1 - a_1)$ and $c_0 = (b_0 + a_0)$

B. RIMC CONTROLLER

Using the repositioning parameter 'θ' [1], (9) is frequency-shifted as

$$\breve{G}_{ILS}(s) = G_{ILS}(s - \theta) = \frac{\left(\breve{a}_0 - \breve{a}_1 s\right)}{\breve{c}_2 s^2 + \breve{c}_1 s + \breve{c}_0} e^{-\beta s} = \frac{\sum_{i=0}^{1} \breve{a}_i (-s)^i}{\sum_{i=0}^{2} \breve{c}_i s^i} e^{-\beta s} \tag{14}$$

where,

$$\left. \begin{array}{c} \breve{a}_0 = (a_0 + a_1\theta)\, e^{\beta\theta} \\ \breve{a}_1 = a_1 e^{\beta\theta} \\ \breve{c}_2 = c_2 \\ \breve{c}_1 = (c_1 - 2\theta c_2) \\ \breve{c}_0 = \left(c_2\theta^2 - \theta c_1 + c_0\right) \end{array} \right\} \tag{15}$$

Applying IMC design principle on (14) instead of (9) results in a RIMC design. The C_{RIMC} [1] is given as

$$C_{RIMC}(s) = \frac{G_f(s)}{\left\{\breve{G}_{ILS}(s)\right\}^-} \tag{16}$$

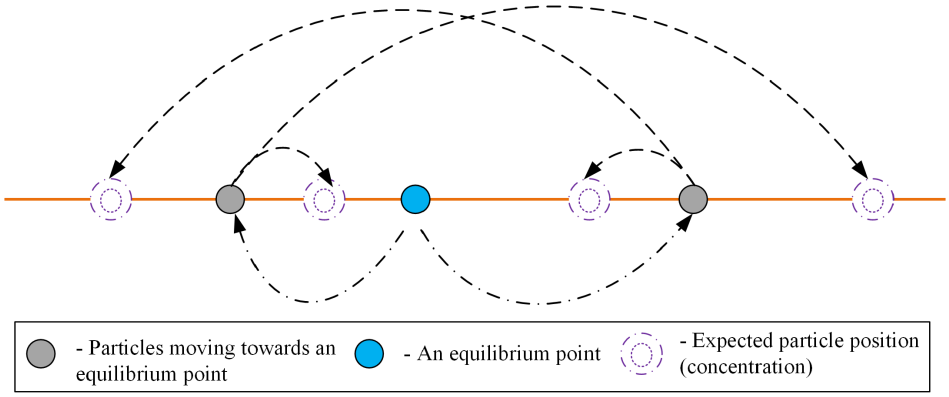

FIGURE 3. The transition of particles in solution space.

where, $\left\{\breve{G}_{ILS}(s)\right\}^{-}$ is the invertible component of $\breve{G}_{ILS}(s)$ and $G_f(s)$ is the low-pass filter with tunable parameters λ_1 and λ_2. $G_f(s)$ is given by

$$G_f(s) = \frac{(\lambda_1 s + 1)}{(\lambda_2 s + 1)^n}, \quad n = 1, 2 \tag{17}$$

The choice of n depends on the order of G. Using (17) in (16) gives

$$C_{RIMC}(s) = \frac{\left(\breve{c}_2 s^2 + \breve{c}_1 s + \breve{c}_0\right)(\lambda_1 s + 1)}{(\lambda_2 s + 1)^n} \tag{18}$$

The repositioning parameter θ serves as the robustness argument. Its selection is vital to establish the robustness/performance tradeoff [1]. Based on the rigorous simulation studies convoluted on a wide range of plant models in Verma and Padhy [20], Aryan et al. [49], Kumar and Raja [8] and Aryan et al. [1], the range of θ is recommended as (0.01, 0.1). The optimal selection of K_P, λ and θ is achieved with the EO algorithm which is elaborated on in the next section.

III. EQUILIBRIUM OPTIMIZER ALGORITHM

EO is of a metaheuristic family that is motivated by the physics laws governing the equilibrium states [43]. It flimsies the fundamental conservation of mass during the particle transitional phase. In EO, the particles imply solutions while their concentration infers the locations. The target of the particles is to pursue their way toward the equilibrium location which signifies the optimal solution (refer to Figure 3). According to the mass balancing principle, the accumulation rate is the difference between the input rate and the output rate plus the generation rate inside the control volume. This can be mathematically modeled [43] as

$$V\frac{dC}{dt} = \rho C_{eqb} - \rho C + G_r \tag{19}$$

where V is the control confinement. C is the concentration contained in V. VdC/dt is the rate of mass change within V. ρ is the rate of volumetric surge. C_{eqb} is the concentration at the equilibrium state and G_r is the rate of generation. As shown in Aryan and Raja [2] and Aryan et al. [1], the integral squared error (ISE) index when considered as the objective cost function gives an improved dynamic response as compared to other indices. So, it is chosen to proceed with the EO algorithm. EO comprises steps such as initialization, allotment of equilibrium search agents, exploration and exploitation of search space, generation, updating and finally termination. These steps have been discussed elaborately in Aryan et al. [1]. It is worth mentioning that the proposed framework does not stick to the local minima as the search space is constrained on stability considerations (following relations established in (10)). Some drawbacks of EO include the inability to solve problem on scattering and sensitivity towards initial parameter selection. A brief flowchart of the same with complete controller tuning is depicted in Figure 4.

A. COMPUTATIONAL COMPLEXITY

The computational complexity (O) of an optimization algorithm is represented by a function that relates the algorithm's running time to the problem's input size. The computational complexity for EO [50] is given as follows:

$$\begin{aligned} O(EO) = {} & O(problem\ formulation) + O(initialization) \\ & + O(t(ISE\ Evaluation) + O(t(memory\ saving)) \\ & + O(t(update\ concentration)) \end{aligned} \tag{20}$$

where, big 'O' notation depicts the computational topology. Consequently, overall computational complexity [50] can be described as follows:

$$\begin{aligned} O(EO) &= O(1 + n_p d_m + t_i J n_p + t_i n_p + t_i n_p d_m) \\ &\sim = O(t_i n_p d_m + t_i J n_p) \end{aligned} \tag{21}$$

where, n_p is the number of particles, d_m is dimension, t_i denotes iterations and J is the cost of function evaluation. The values used for the current study are $n_p = 10$, $d_m = 1$ and $t_i = 20$. The simulations are performed on MATLAB and SIMULINK R2020a version on a system with the following specifications: Processor-AMD Ryzen-5 5600H; Clock

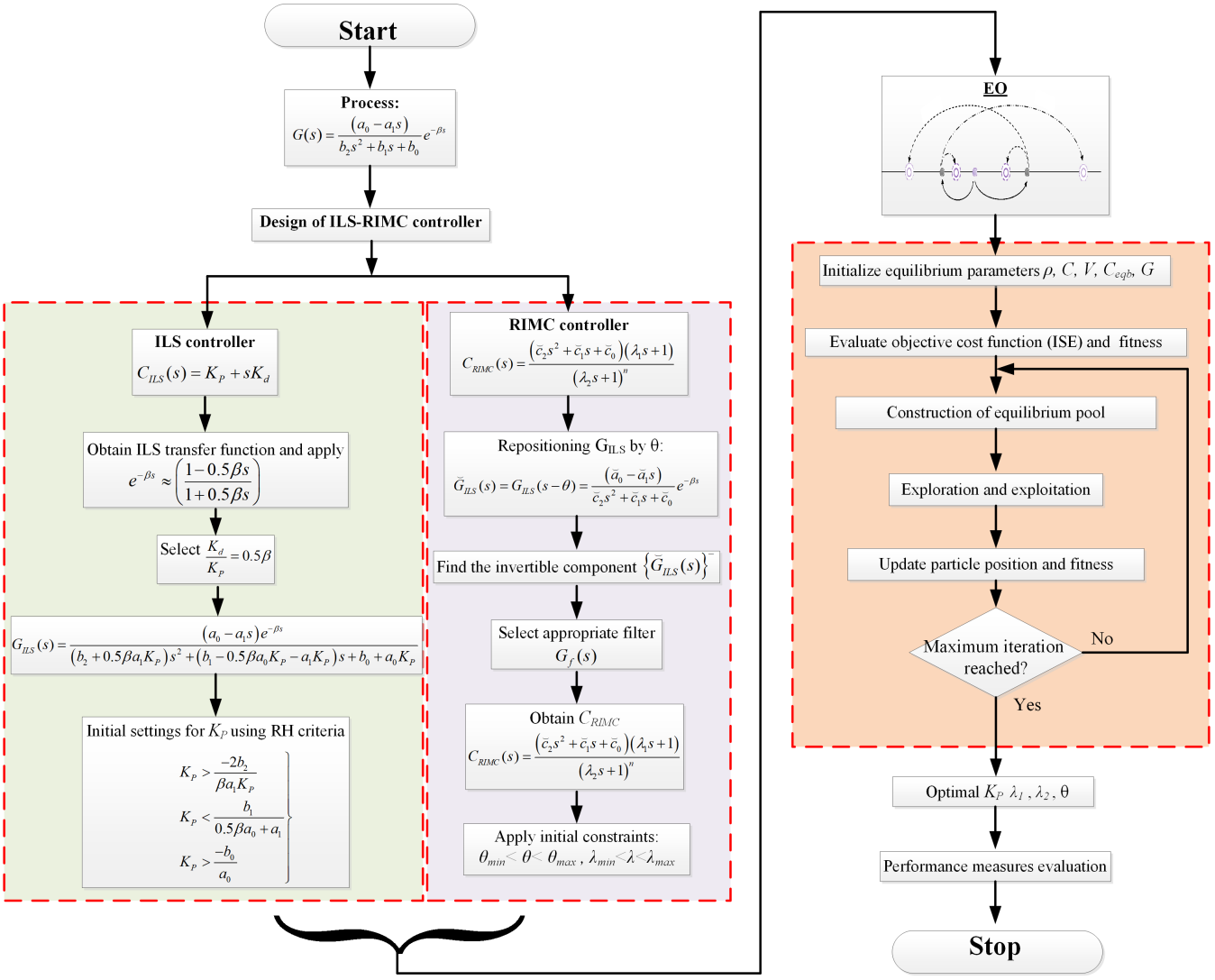

FIGURE 4. EO flowchart with the suggested controller design framework.

speed-3.30 GHz; RAM-8 GB; GPU-4GB. The computational time for both the simulation examples are 264.08 sec and 218.97 sec, respectively.

IV. RESULTS AND DISCUSSION

The recommended ILS-RIMC strategy is tested for its applicability on some benchmark UIPs followed by a case study on CSTR.

A. SIMULATION STUDIES ON BENCHMARK UIPs

The considered plant models with optimized controller settings are given in Table 1. The servo response is achieved by applying the positive unit step 'R' at $t = 0$s while the regulatory response is achieved by applying disturbance 'δ' (refer to Figure 2) at a considerable time after the servo transients have died out. The transient performance metrics such as the absolute peak overshoot ($|\hat{O}|$), absolute peak undershoot ($|\hat{U}|$), settling time (T_{st}) along with integral error measures (*ISE*, *IAE*, *ITSE* and *ITAE*) are evaluated and compared in Table 2. The aforementioned measures are calculated separately for servo and regulatory response except for the time weighted measures (*ITSE* and *ITAE*) which are calculated for the complete response to evaluate the effectiveness of the ILS-RIMC strategy. Since a perfect plant model is impossible, the control scheme must be subjected to an imperfect (perturbed) model to evaluate its robustness. For perturbed analysis, the plant (G) parameters (a_i, b_i and β in (1)) are changed up to 30% (positive change in a_i and β; negative change in b_i) while the controller settings remain the same as that of the nominal case.

1) EXAMPLE 1

Boilers are used to convert water into steam for downstream equipment. When the boiler is running, steam is constantly

TABLE 1. Process models and settings for simulation.

Ex	$G(s)$	Work	Settings
1	$\frac{0.547(-0.418s+1)}{s(1.06s+1)}e^{-0.1s}$	Raja and Ali [7]	$K_p=-0.259, T_i=-1.386, K_C=1.3, T_D=0.05$
		Raja [47]	$K_p=-0.077, T_i=-0.372, K_C=1.3, T_D=0.05$
		Proposed1 and Proposed2	$K_p=1.012, \lambda=0.923, \theta=0.011$ and $K_p=1, \lambda=0.9, \theta=0.01$
2	$\frac{-0.173(1-4.473s)}{(3.1s-1)}$	Sree and Chidambaram [10]	$C(s)=-4.8615/\left(1+{}^{1}/_{-128.08s}\right)$
		Raja and Ali [7]	$K_p=-4.8, K_C=0.229, T_D=2.409$
		Kumari et al. [5]	$C(s)=(-0.61s-0.1696)/(-0.173)\left(1+12s^{1.1}\right)^2, Kp=-4.8$
		Proposed	$K_p=-4.76, \lambda=13.05, \theta=0.0131$

TABLE 2. Comparison of various performance indicators without perturbation.

Ex	Work	$\hat{O}/\hat{U}$		T_{st}		IAE		ISE		ITAE	ITSE
		Servo	Reg.	Servo	Reg.	Servo	Reg.	Servo	Reg.		
1	Raja and Ali [7]	1.000	0.954	18.09	67.58	6.281	4.92	4.424	3.121	309.5	186.3
	Raja [47]	1.000	1.039	18.99	69.08	7.058	5.685	5.739	4.052	355.4	244.8
	Proposed1	1.006	**0.703**	**5.41**	65.18	**2.167**	**2.928**	**1.660**	**1.352**	**165.2**	**75.92**
	Proposed2	1.006	0.725	9.90	**64.61**	2.226	2.976	1.653	1.411	168.7	79.06
2	Sree and Chidambaram [10]	5.731	2.166	74.151	182.51	246.1	192.5	890.1	658.5	7843	14420
	Raja and Ali [7]	1.000	2.770	17.251	151.53	14.52	31.11	10.22	22.01	2182	1447
	Kumari et al. [5]	1.000	2.724	17.560	148.22	13.44	29.12	9.910	20.00	2391	1398
	Proposed	1.000	2.467	20.123	157.41	13.57	30.18	10.34	20.71	2421	1452

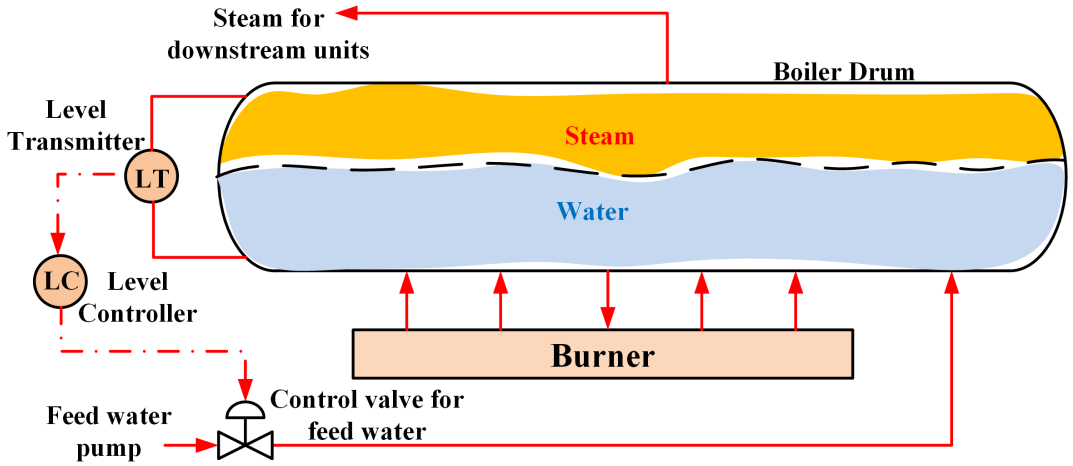

FIGURE 5. Liquid level tracking in boiler steam drum [9].

visible above the water layer. These steam bubbles condense as feed water (which is much below the boiling point) is added, temporarily lowering the drum level [9]. This NMP behavior is quickly reversed by increased feed-water inflow. For this boiler steam level control system, the drum level is considered as the system output while the flow rate of feed water is the control effort (refer to Figure 5). This operation was modeled by Raja and Ali [7] as an inverse response I2PTD process model given by

$$G(s)=\frac{0.547\,(-0.418s+1)}{s\,(1.06s+1)}e^{-0.1s} \tag{22}$$

Raja and Ali [7] and Raja [47] designed the DCL schemes (PI-PD in [7] and SP-based PI-PD in [47]) for (22). The controller settings of the aforementioned techniques are given in Table 1. To analyze the disturbance rejection, $\delta=-1$ is added at $t=50$s. The ILS controller constructed on Pade's first-order and second-order approximations (as deliberated in section II-A) are labeled as 'Proposed1' and 'Proposed2' respectively. The suggested ILS-RIMS strategy yields superior servo response as compared to DCL strategies of [7] and [47] for the nominal case (refer to Figure 7(a)). This is also vindicated in the T_{st} values of Table 2. The disturbance rejection capability of ILS-RIMC is much better than the above-cited DCL methods with the former giving a significantly lesser $|\hat{U}|$. With 20% perturbation, the process model is modified as $G_0(s)=0.6564e^{-0.12s}\,(-0.5016s+1)\,/s\,(0.848s+1)$. The responses with are shown in Figures 6(c) and 6(d). Like the nominal case, the ILS-RIMC strategy once again delivers an improved response than the other two methods. Furthermore, ILS-RIMC is capable of handling perturbations

TABLE 3. Comparison of integral measures for various perturbation levels.

Ex	Perturbation	$G_0(s)$	Work	IAE		ISE		ITAE	ITSE
				Servo	Reg.	Servo	Reg.		
1	10%	$\frac{0.6017(-0.4598s+1)}{s(0.954s+1)}e^{-0.11s}$	Raja and Ali [7]	6.281	4.911	4.323	3.211	309.5	190.0
			Raja [47]	7.057	5.586	5.624	4.128	349.7	247.0
			Proposed1	**2.216**	**2.598**	**1.597**	**1.359**	**145.9**	**75.56**
			Proposed2	2.268	2.677	1.603	1.465	151.0	79.67
	20%	$\frac{0.6564(-0.5016s+1)}{s(0.848s+1)}e^{-0.12s}$	Raja and Ali [7]	6.281	4.951	4.240	3.344	312.2	196.3
			Raja [47]	7.057	5.553	5.532	4.231	348.0	251.1
			Proposed1	**2.254**	**2.351**	**1.598**	**1.396**	**132.0**	**77.17**
			Proposed2	2.358	2.538	1.628	1.501	143.8	82.96
	30%	$\frac{0.7111(-0.5434s+1)}{s(0.742s+1)}e^{-0.13s}$	Raja and Ali [7]	6.281	5.073	4.172	3.551	319.8	206.8
			Raja [47]	7.057	5.563	5.459	4.375	348.7	257.5
			Proposed1	**2.580**	**2.500**	**1.739**	**1.516**	**143.4**	**83.9**
			Proposed2	2.938	2.862	1.833	1.689	168.1	93.9
2	10%	$\frac{-0.1903(1-4.903s)}{(2.79s-1)}$	Sree and Chidambaram [10]	310.0	212.5	1002	710.1	3.5×10^4	9.4×10^4
			Raja and Ali [7]	17.73	33.11	13.14	24.47	7411	3907
			Kumari et al. [5]	18.54	34.10	14.07	24.40	8070	4272
			Proposed	**17.26**	**33.49**	**14.31**	**24.23**	5696	3290
	20%	$\frac{-0.2076(1-5.367s)}{(2.48s-1)}$	Sree and Chidambaram [10]	401.4	278.4	-	-	2.7×10^5	5.1×10^6
			Raja and Ali [7]	22.71	38.22	19.74	29.29	7.7×10^4	4.5×10^5
			Kumari et al. [5]	23.64	37.17	18.12	29.51	1.2×10^5	1.1×10^6
			Proposed	22.84	38.19	**18.12**	**28.33**	3.0×10^4	6.1×10^4

as high as 30% with satisfactorily enhanced performance measures (refer to Table 3). It is worth mentioning that both 'Proposed1' and 'Proposed2' ILS controllers produce fairly similar responses due to less value of β (0.1 in this case). For higher β systems, Pade's second-order approximation is recommended [48].

2) EXAMPLE 2

Sree and Chidambaram [10] have studied an enzymatic bioreactor (Figure 7) expressed by the following relation:

$$\frac{dC_c}{dt} = \left[\frac{n_1 Q}{n_2 V}\right](C_{flow} - C_c) - \frac{k_1 C_c}{(k_2 C_c + 1)^2} \tag{23}$$

where C_c is the concentration of the uniformly stirred region. Blend concentration (at the outlet) is indicated as C_{out} subject to the following continuity expression [9]:

$$n_1 C_c = (1 - n_1) C_{flow} + C_{out} \tag{24}$$

The parameters in (23) and (24) have the following values: $n_1 = n_2 = 0.75$, $(k_1 V)/Q = 300$, $k_1 = 10s^{-1}$, $k_2 = 1\ dm^3\ kmol^{-1}$, $V = 1dm^3$ [9]. Considering the deviation in C_{out} as the process output and change in C_{flow} as the control effort along with the operating conditions ($C_{flow} = 6.48\ kmol^3$ and $C_{out} = 1.8kmol^3$), the linear model [10] is attained as

$$G(s) = \frac{-0.173(1 - 4.473s)}{(3.1s - 1)} \tag{25}$$

For the NMP process model (25), Sree and Chidambaram [10] designed a unity feedback PI controller while Kumari et al. [5] and Raja and Ali [7] suggested DCL strategies. Reference [5] devised a fractional-order IMC-P strategy while Raja and Ali [7] employed the PI-PD scheme. The controller settings of the aforementioned techniques are given in Table 1. To analyze the disturbance rejection, $\delta = -1$ is added at $t = 125$s. Since in this study, $\beta = 0$, no approximation was required in the G_{ILS} expression (given in (5)). The servo response of [10] produces large $|\hat{U}|$ before settling. Though the suggested ILS-RIMC scheme yields comparable performance as that of [5] and [7] for the nominal case (refer to Figure 8(a) and 8(b)), the former outperforms the latter schemes for higher levels of perturbation as noted in Table 3. For 20% perturbation, the plant model is modified as $G_0(s) = -0.2076(1 - 5.3676s)/(2.48s - 1)$. The responses for this case are shown in Figures 7(c) and 7(d). The ILS-RIMC strategy produces lesser $|\hat{U}|$ than [5] and [7] with relatively lower control efforts.

B. ROBUST STABILITY ANALYSIS

To examine the ILS-RIMC controller for robustness towards uncertainties in the approximated model ($G_o(j\omega)$), the following closed-loop robust stability condition [1] is explored:

$$T(j\omega) G_{CS}(j\omega) < 1 \quad \forall\omega \in (-\infty, \infty) \tag{26}$$

where, $G_{CS}(j\omega)$ is the closed-loop complementary sensitivity and $T_{UN}(j\omega)$ is the uncertainty norm of the plant model. $T_{UN}(j\omega)$ is given [1] by

$$T_{UN}(j\omega) = \left|\frac{G_o(j\omega) - G(j\omega)}{G_o(j\omega)}\right| \tag{27}$$

Taking into account uncertainties of a_i, b_i and β as Δa_i, Δb_i and $\Delta\beta$ in (24), (23) becomes

$$\|G_{CS}(j\omega)\|_\infty < \left|\frac{\left(1 - \frac{j\omega\Delta b_i}{j\omega b_i + 1}\right)}{\left\{\left(1 - \frac{\Delta a_i}{a_i}\right)e^{-j\omega\Delta\beta} - \left(1 - \frac{j\omega\Delta b_i}{j\omega b_i + 1}\right)\right\}}\right| \quad \forall\omega > 0 \tag{28}$$

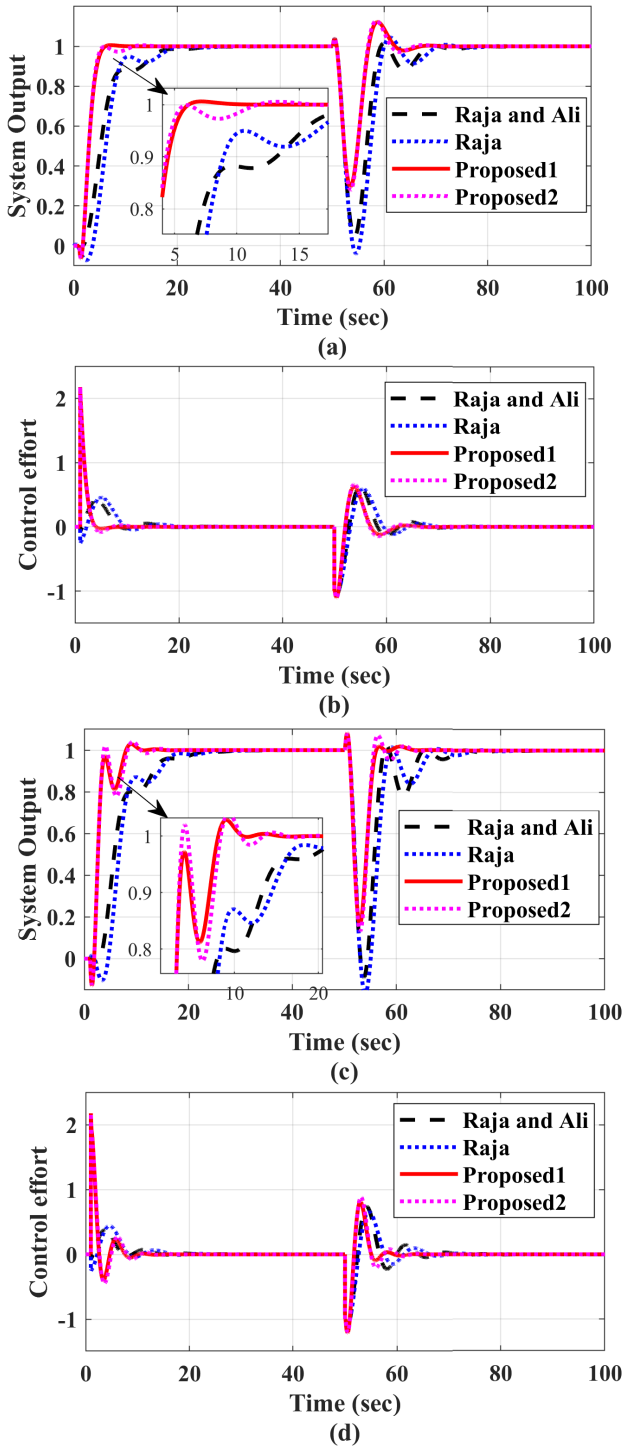

FIGURE 6. Plots for example-1: Comparison of (a) system output with nominal plant parameters (b) nominal control efforts (c) system output with 20% perturbed plant parameters (d) perturbed control efforts.

For an uncertainty of 20%, bode magnitude plots (for $G_{CS}(j\omega)$ and $T_{UN}(j\omega)$) are given in Figure 9. It can be observed that the inequality relation of (28) is fulfilled for all the examples thereby satisfying the condition for robust stability.

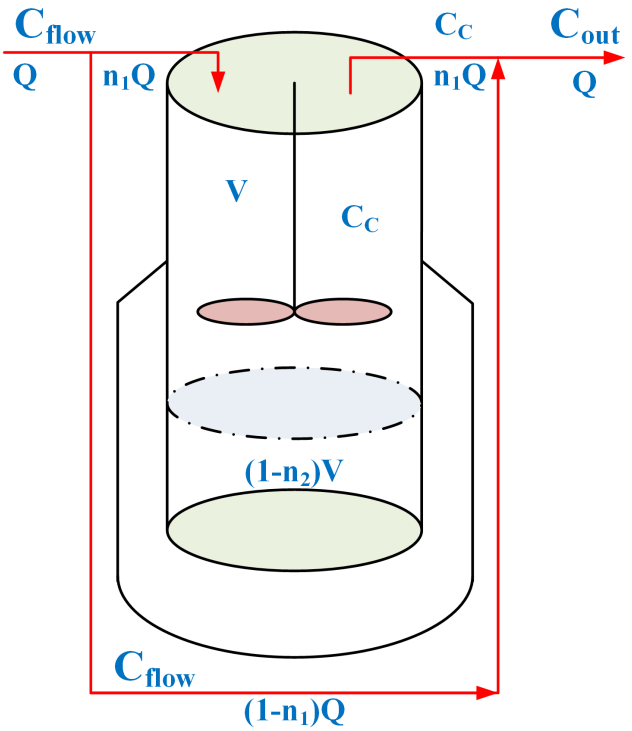

FIGURE 7. Enzymatic reactor subjected to continuous mixing.

TABLE 4. Parameters of Jacketed CSTR [51].

C_P - Concentration of P component
$\Delta\theta$ - Generated heat of reaction $= 50,000$ kJ/kmol
C_{PF} - Feed concentration $= 7.5$kmol/m^3
σ - Density of components $= 850$ kg/m^3
F_X- Reactor feed flow rate $= 0.00065$ m^3/s
$C_\theta-$ Specific heat $= 3.5$ kJ/(kgK)
V- Control volume $= 1$ m^3
χ - Coefficient of heat transfer $= 1.4$ kJ/(sK)
r_X- Reaction rate
A_θ - Area of heat transfer
C_Q - Concentration of Q component
K- Decay constant $= 1.8 \times 10^7$ s^{-1}
T_{r-} Reactor temperature
E_A- Activation energy $= 69000$ kJ/kmol
T_F - Feed temperature $= 300$ K
R- Gas constant $= 8.345$ kJ/(kmolK)

C. CASE STUDY ON JACKETED CSTR

A CSTR setup is shown in Figure 10(a). Temperature control is a critical aspect of jacketed-type CSTR [8], [51]. Consider an exothermic, irreversible first-order reaction P to Q in a CSTR. The jacket dynamics are neglected for controller design purposes [51]. The dynamic equations that govern this process [8] are given as follows:

$$\frac{dC_P}{dt} = (C_{PF} - C_P)\frac{F_X}{V} - r_X \tag{29}$$

$$\frac{dC_Q}{dt} = -C_Q\frac{F_X}{V} + r_X \tag{30}$$

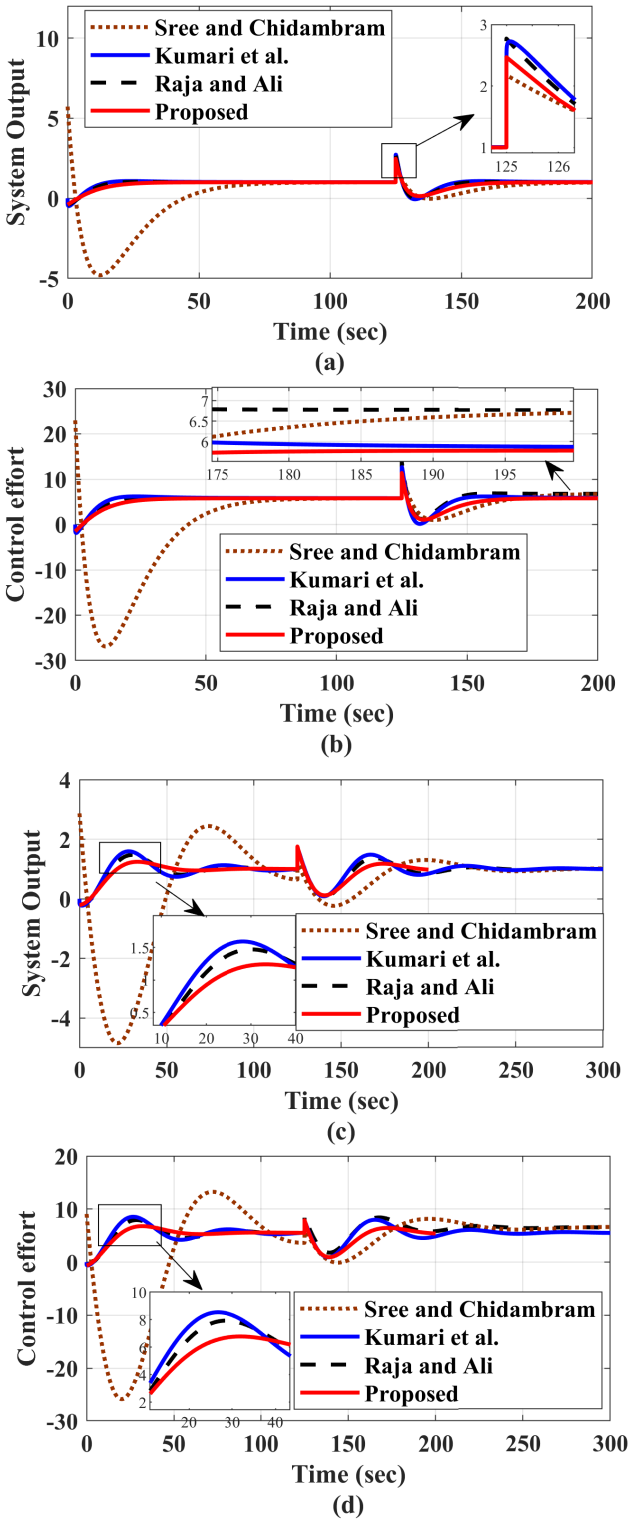

FIGURE 8. Plots for example-2: Comparison of (a) system output with nominal plant parameters (b) nominal control efforts (c) system output with 20% perturbed plant parameters (d) perturbed control efforts.

$$\frac{dT_r}{dt} = (T_F - T_r)\frac{F_X}{V} - \frac{\Delta\theta r_X}{\sigma C_\theta} - \frac{\chi A_\theta}{\sigma V C_\theta}(T_r - T_C) \quad (31)$$

$$r_X = K C_P e^{-E_A/RT_r} \quad (32)$$

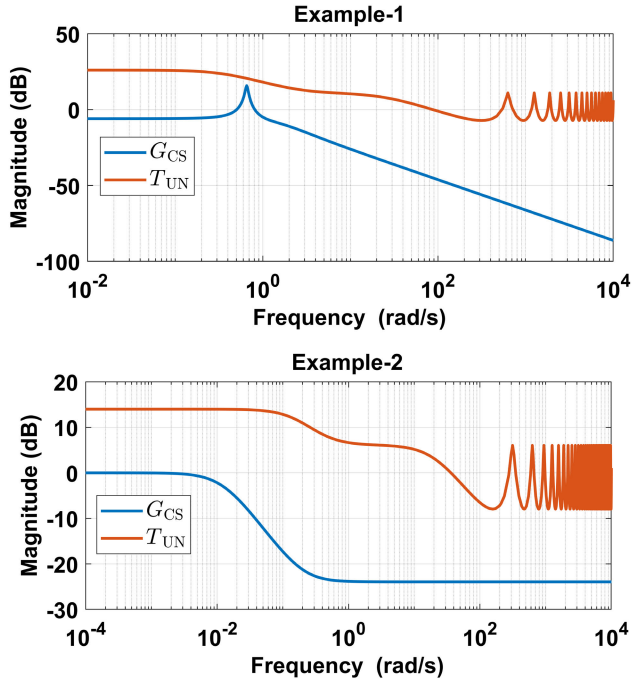

FIGURE 9. Bode plots (magnitude) of $G_{CS}(j\omega)$ and $T_{UN}(j\omega)$ for both examples.

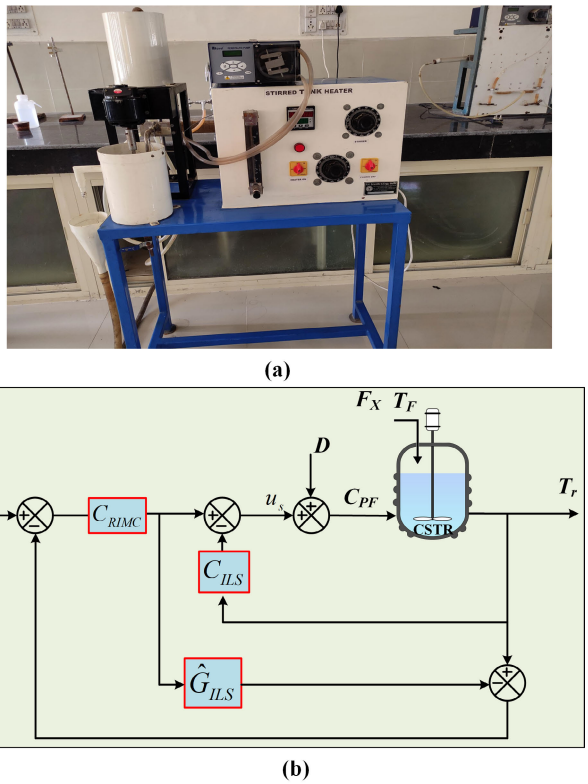

FIGURE 10. Simulation using CSTR model (a) An example of CSTR setup (b) ILS-RIMC scheme for CSTR.

The parameters used in (29)-(32) are listed in Table 4. This reactor's mathematical model is non-linear which is

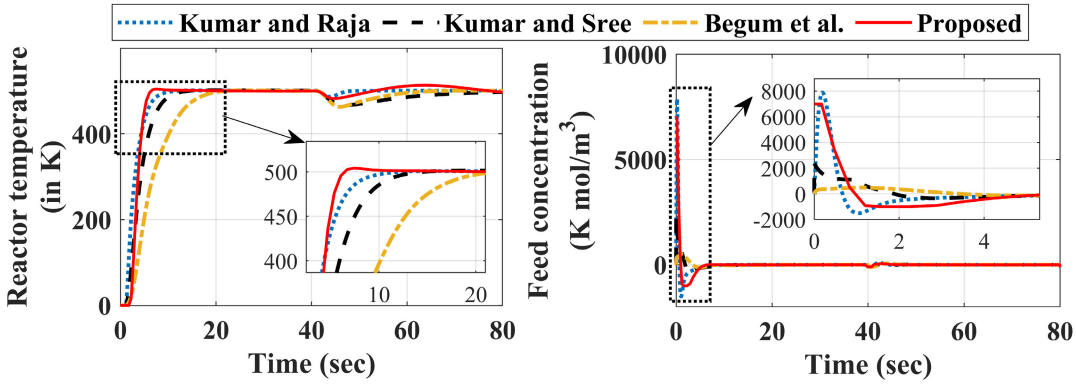

FIGURE 11. Plots of CSTR response.

linearized as follows [8]:

$$G(s) = \frac{T_r(s)}{C_{PF}(s)} = \frac{0.9693e^{-s}}{s(12.422s+1)} \tag{33}$$

The temperature set-point is set at $T_{st} = 500K$. In the simulation (refer to Figure 10(b)), a disturbance of $D = -100$ is supplied to the process at t=40 sec. The ILS-RIMC settings are obtained using the procedure delivered in section-II (for Pade's first order approximation) as $K_P = 0.2501$, $\theta = 0.0102$ and $\lambda_2 = 0.701$. The suggested method is compared with other works on CSTR temperature control (Kumar and Raja [8] Kumar and Sree [52] Begum et al. [23]). The details of the controller settings of these works can be found in [8]. The plots of plant output (reactor temperature) and control efforts (feed concentration) are shown in Figure 11. It is evident that the suggested strategy is capable of handling this challenging CSTR model with a satisfactorily enhanced response as compared to other works.

V. CONCLUSION

This work explores the application of repositioned internal model controller (RIMC) on inverse response integrating/unstable processes with dead-time using inner-loop stabilization (ILS) and equilibrium optimizer. The ILS is achieved by utilizing a proportional-derivative (PD) controller subjected to Routh Hurwitz stability criteria. The repositioning parameter helps to achieve a desired performance/robustness tradeoff which is illustrated with benchmark plants such as boiler drum, enzymatic reactor and continuously stirred tank reactor. The suggested strategy is also subjected to robust stability analysis. It provides an appreciable improvement in the dynamic response to step reference change and disturbance introduction which is reflected in enhanced transient and steady-state measures as compared to some of the relevant works. In future, better heuristic algorithm can be used which can overcome the drawbacks of EO such as scattering and sensitivity towards initial parameter selection. The closed-loop performance of the suggested design can be further enhanced if the control structure is modified such that the servo and regulatory responses are decoupled.

REFERENCES

[1] P. Aryan, G. L. Raja, and R. Vilanova, "Experimentally verified optimal bi-loop re-located IMC strategy for unstable and integrating systems with dead time," *Int. J. Syst. Sci.*, vol. 54, no. 7, pp. 1–19, 2023.
[2] P. Aryan and G. L. Raja, "A novel equilibrium optimized double-loop control scheme for unstable and integrating chemical processes involving dead time," *Int. J. Chem. React. Eng.*, vol. 20, no. 12, pp. 1341–1360, Dec. 2022.
[3] U. Mehta, P. Aryan, and G. L. Raja, "Tri-parametric fractional-order controller design for integrating systems with time delay," *IEEE Trans. Circuits Syst. II, Exp. Briefs*, early access, Apr. 25, 2023, doi: 10.1109/TCSII.2023.3269819.
[4] D. Kumar, P. Aryan, and G. L. Raja, "Design of a novel fractional-order internal model controller-based Smith predictor for integrating processes with large dead-time," *Asia–Pacific J. Chem. Eng.*, vol. 17, no. 1, p. e2724, 2022.
[5] S. Kumari, P. Aryan, and G. L. Raja, "Design and simulation of a novel FOIMC-PD/P double-loop control structure for CSTRs and bioreactors," *Int. J. Chem. React. Eng.*, vol. 19, no. 12, pp. 1287–1303, Dec. 2021.
[6] A. Mahmood, A. Q. Khan, G. Mustafa, N. Ullah, M. Abid, and A. S. Khan, "Remote fault-tolerant control for industrial smart surveillance system," *Math. Problems Eng.*, vol. 2021, pp. 1–12, Jun. 2021.
[7] G. Lloyds Raja and A. Ali, "New PI-PD controller design strategy for industrial unstable and integrating processes with dead time and inverse response," *J. Control, Autom. Electr. Syst.*, vol. 32, no. 2, pp. 266–280, Apr. 2021.
[8] D. Kumar and G. L. Raja, "Unified fractional indirect IMC-based hybrid dual-loop strategy for unstable and integrating type CSTRs," *Int. J. Chem. React. Eng.*, vol. 21, no. 3, pp. 251–272, Mar. 2023.
[9] G. L. Raja, "Robust I-PD controller design with case studies on boiler steam drum and bioreactor," in *Proc. 15th Int. Conf. Comput. Autom. Eng. (ICCAE)*, Mar. 2023, pp. 486–491.
[10] R. P. Sree and M. Chidambaram, "Control of unstable bioreactor with dominant unstable zero," *Chem. Biochem. Eng. Quart.*, vol. 17, no. 2, pp. 139–146, 2003.
[11] A. Seshagiri Rao, V. S. R. Rao, and M. Chidambaram, "Direct synthesis-based controller design for integrating processes with time delay," *J. Franklin Inst.*, vol. 346, no. 1, pp. 38–56, Feb. 2009.
[12] B. Vanavil, K. K. Chaitanya, and A. S. Rao, "Improved PID controller design for unstable time delay processes based on direct synthesis method and maximum sensitivity," *Int. J. Syst. Sci.*, vol. 46, no. 8, pp. 1349–1366, 2015.
[13] M. Ajmeri, "Analytical design of enhanced PID controller with set-point filter for unstable processes with time delay," *Int. J. Dyn. Control*, vol. 11, pp. 1–10, Jul. 2022.
[14] R. Vilanova and A. Visioli, *PID Control in the Third Millennium*. London, U.K.: Springer, 2012.
[15] O. Arrieta, R. Vilanova, and A. Visioli, "Proportional-integral-derivative tuning for servo/regulation control operation for unstable and integrating processes," *Ind. Eng. Chem. Res.*, vol. 50, no. 6, pp. 3327–3334, Mar. 2011.

[16] D. C. Babu, D. B. S. Kumar, and R. P. Sree, "Tuning of PID controllers for unstable systems using direct synthesis method," *Indian Chem. Engineer*, vol. 59, no. 3, pp. 215–241, Jul. 2017.

[17] A. Ali and S. Majhi, "PID controller tuning for integrating processes," *ISA Trans.*, vol. 49, no. 1, pp. 70–78, Jan. 2010.

[18] R. C. Panda, "Synthesis of PID controller for unstable and integrating processes," *Chem. Eng. Sci.*, vol. 64, no. 12, pp. 2807–2816, Jun. 2009.

[19] B. Vanavil, A. V. N. L. Anusha, M. Perumalsamy, and A. S. Rao, "Enhanced IMC-PID controller design with lead-lag filter for unstable and integrating processes with time delay," *Chem. Eng. Commun.*, vol. 201, no. 11, pp. 1468–1496, Nov. 2014.

[20] B. Verma and P. K. Padhy, "Indirect IMC-PID controller design," *IET Control Theory Appl.*, vol. 13, no. 2, pp. 297–305, 2019.

[21] M. Irshad and A. Ali, "IMC based robust PI/PID controllers for time-delayed inverse response processes," *ISA Trans.*, vol. 134, pp. 278–289, Mar. 2023.

[22] R. Vilanova, "IMC based robust PID design: Tuning guidelines and automatic tuning," *J. Process Control*, vol. 18, no. 1, pp. 61–70, Jan. 2008.

[23] K. G. Begum, A. S. Rao, and T. K. Radhakrishnan, "Enhanced IMC based PID controller design for non-minimum phase (NMP) integrating processes with time delays," *ISA Trans.*, vol. 68, pp. 223–234, May 2017.

[24] J. H. Park, S. W. Sung, and I.-B. Lee, "An enhanced PID control strategy for unstable processes," *Automatica*, vol. 34, no. 6, pp. 751–756, Jun. 1998.

[25] V. Vijayan and R. C. Panda, "Design of PID controllers in double feedback loops for SISO systems with set-point filters," *ISA Trans.*, vol. 51, no. 4, pp. 514–521, Jul. 2012.

[26] E.-D. Cong, M.-H. Hu, S.-T. Tu, F.-Z. Xuan, and H.-H. Shao, "A novel double loop control model design for chemical unstable processes," *ISA Trans.*, vol. 53, no. 2, pp. 497–507, Mar. 2014.

[27] M. Ajmeri and A. Ali, "Two degree of freedom control scheme for unstable processes with small time delay," *ISA Trans.*, vol. 56, pp. 308–326, May 2015.

[28] HongboZou and H. Li, "Tuning of PI–PD controller using extended non-minimal state space model predictive control for the stabilized gasoline vapor pressure in a stabilized tower," *Chemometric Intell. Lab. Syst.*, vol. 142, pp. 1–8, Mar. 2015.

[29] C. Onat, "A new design method for PI–PD control of unstable processes with dead time," *ISA Trans.*, vol. 84, pp. 69–81, Jan. 2019.

[30] F. Alyoussef and I. Kaya, "Proportional–integral and proportional–derivative controller design based on analytically computed centroid point for controlling integrating processes," *Proc. Inst. Mech. Eng., I, J. Syst. Control Eng.*, Jan. 2023, Art. no. 09596518221143815.

[31] F. Alyoussef and I. Kaya, "Simple PI-PD tuning rules based on the centroid of the stability region for controlling unstable and integrating processes," *ISA Trans.*, vol. 134, pp. 238–255, Mar. 2023.

[32] I. Kaya and F. Peker, "Optimal I-PD controller design for setpoint tracking of integrating processes with time delay," *IET Control Theory Appl.*, vol. 14, no. 18, pp. 2814–2824, Dec. 2020.

[33] S. Chakraborty, S. Ghosh, and A. K. Naskar, "I–PD controller for integrating plus time-delay processes," *IET Control Theory Appl.*, vol. 11, no. 17, pp. 3137–3145, Nov. 2017.

[34] T. Dogruer, "Design of I-PD controller based modified Smith predictor for processes with inverse response and time delay using equilibrium optimizer," *IEEE Access*, vol. 11, pp. 14636–14646, 2023.

[35] D. Kumar, P. Aryan, and G. L. Raja, "Decoupled double-loop FOIMC-PD control architecture for double integral with dead time processes," *Can. J. Chem. Eng.*, vol. 100, no. 12, pp. 3691–3703, 2022.

[36] S. Mirjalili, S. M. Mirjalili, and A. Lewis, "Grey wolf optimizer," *Adv. Eng. Softw.*, vol. 69, pp. 46–61, Mar. 2014.

[37] S. Mirjalili, "SCA: A sine cosine algorithm for solving optimization problems," *Knowl.-Based Syst.*, vol. 96, pp. 120–133, Mar. 2016.

[38] S. Mirjalili, "Moth-flame optimization algorithm: A novel nature-inspired heuristic paradigm," *Knowl.-Based Syst.*, vol. 89, pp. 228–249, Nov. 2015.

[39] I. Ahmed, A. R. Rao, A. Shah, E. Alamzeb, and J. A. Khan, "Performance of various metaheuristic techniques for economic dispatch problem with valve point loading effects and multiple fueling options," *Adv. Electr. Eng.*, vol. 2014, pp. 1–14, Nov. 2014.

[40] I. Ahmed, M. Rehan, A. Basit, and K.-S. Hong, "Greenhouse gases emission reduction for electric power generation sector by efficient dispatching of thermal plants integrated with renewable systems," *Sci. Rep.*, vol. 12, no. 1, p. 12380, Jul. 2022.

[41] I. Ahmed, U.-E.-H. Alvi, A. Basit, M. Rehan, and K.-S. Hong, "Multi-objective whale optimization approach for cost and emissions scheduling of thermal plants in energy hubs," *Energy Rep.*, vol. 8, pp. 9158–9174, Nov. 2022.

[42] I. Ahmed, U.-E.-H. Alvi, A. Basit, T. Khursheed, A. Alvi, K.-S. Hong, and M. Rehan, "A novel hybrid soft computing optimization framework for dynamic economic dispatch problem of complex non-convex contiguous constrained machines," *PLoS ONE*, vol. 17, no. 1, Jan. 2022, Art. no. e0261709.

[43] A. Faramarzi, M. Heidarinejad, B. Stephens, and S. Mirjalili, "Equilibrium optimizer: A novel optimization algorithm," *Knowl.-Based Syst.*, vol. 191, Mar. 2020, Art. no. 105190.

[44] P. Aryan and G. L. Raja, "Design and analysis of novel QOEO optimized parallel fuzzy FOPI-PIDN controller for restructured AGC with HVDC and PEV," *Iranian J. Sci. Technol., Trans. Electr. Eng.*, vol. 46, no. 2, pp. 565–587, Jun. 2022.

[45] H. Shukla and M. Raju, "Combined frequency and voltage regulation in multi-area system using an equilibrium optimiser based non-integer controller with penetration of electric vehicles," *Int. J. Ambient Energy*, pp. 1–27, Feb. 2023.

[46] R. Shivhare, N. Rastogi, M. Bhardwaj, E. Kumari, N. Agrawal, and M. Jain, "Precise temperature control scheme for nonlinear CSTR using equilibrium optimizer tuned 2-DOF FOPID controller," in *Computational Intelligence: Select Proceedings of InCITe*. London, U.K.: Springer, 2023, pp. 93–104.

[47] G. L. Raja, "Enhanced design of a PI-PD based Smith predictor for industrial plants," *IFAC-PapersOnLine*, vol. 54, no. 21, pp. 79–84, 2021.

[48] M. Vajta, "Some remarks on Padé-approximations," in *Proc. 3rd TEMPUS-INTCOM Symp.*, vol. 242, 2000, pp. 1–6.

[49] P. Aryan, G. L. Raja, and R. Vilanova, "Optimal iIMC-PD double-loop control strategy for integrating processes with dead-time," in *Proc. 15th APCA Int. Conf. Autom. Control Soft Comput. (CONTROLO)*. Caparica, Portugal: Springer, Jul. 2022, pp. 521–531.

[50] *A Novel Physics Based Optimization Algorithm: Equilibrium Optimizer (EO)*. Accessed: May 10, 2023. [Online]. Available: https://transpireonline.blog/2020/03/20/a-novel-physics-based-optimization-algorithm-equilibrium-optimizer-eo/

[51] R. A. Wright and C. Kravaris, "Two-degree-of-freedom output feedback controllers for discrete-time nonlinear systems," *Chem. Eng. Sci.*, vol. 61, no. 14, pp. 4676–4688, Jul. 2006.

[52] D. B. S. Kumar and R. P. Sree, "Tuning of IMC based PID controllers for integrating systems with time delay," *ISA Trans.*, vol. 63, pp. 242–255, Jul. 2016.

PULAKRAJ ARYAN (Graduate Student Member, IEEE) received the bachelor's degree in electrical and electronics engineering from the Birla Institute of Technology, Mesra, Ranchi, India, in 2016, and the master's degree from the National Institute of Technology Patna, India, in 2020, where he is currently pursuing the Ph.D. degree in control systems. He has authored several book chapters and has more than 17 publications in peer-reviewed international conference proceedings and reputed journals. His current research interest includes optimal control strategies for industrial processes.

G. LLOYDS RAJA (Member, IEEE) received the bachelor's degree in electronics and communication engineering and the master's degree in embedded system technologies from Anna University, in 2009 and 2011, respectively, and the Ph.D. degree from the Electrical Engineering Department, Indian Institute of Technology Patna, in 2018. From 2017 to 2020, he was an Assistant Professor with the Kalinga Institute of Industrial Technology. He visited the Department of Automation, Shanghai Jiao Tong University, China, as a Postdoctoral Researcher, for a short duration. Since 2020, he has been with the Electrical Engineering Department, National Institute of Technology Patna, where he is currently an Assistant Professor. He has edited two books on control engineering, authored several book chapters, and has more than 37 publications in peer-reviewed international conference proceedings and reputed journals. His current research interests include chemical process control, advanced load frequency control strategies, adaptive control, and applications of metaheuristic optimization techniques for controller tuning. He is a member of IFAC-ACDOS.

RAMON VILANOVA (Member, IEEE) received the degree and Ph.D. degree from the Autonomous University of Barcelona, in 1991 and 1996, respectively. He is currently a Full Professor of automatic control and systems engineering with the School of Engineering, Autonomous University of Barcelona, where he teaches subjects, such as signals and systems, and automatic control and technology of automated systems. He is the author of several book chapters and has more than 100 publications in international congresses/journals. His research interests include methods of tuning PID regulators, systems with uncertainty, analysis of control systems with several degrees of freedom, application to environmental systems, and development of methodologies for the design of machine–man interfaces. He is a member of IFAC and IEEE-IES.

MONTSE MENESES (Member, IEEE) received the Ph.D. degree in chemical engineering from Universitat Rovira i Virgili (URV), Spain, in 2002.

From 2002 to 2006, she was an Environmental Technician with Centre d'Innovació Química, URV, after which she continued as an Associate Professor with URV, in 2007. Since 2018, she has been an Associate Professor with Telecomunicació i Enginyeria de Sistemes, Autonomous University of Barcelona (UAB), Spain. She has worked on more than ten government-funded research projects as a principal investigator and a contributor which are published in reputed international congresses/journals. Her current research interests include environmental engineering, life cycle assessment, and environmental impact.